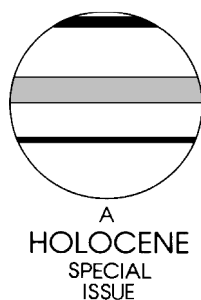


Theoretical equilibrium-line altitudes and glacier buildup sensitivity in southern Norway based on meteorological data in a geographical information system

Øyvind Lie,^{1,3,*} Svein Olaf Dahl^{2,3} and Atle Nesje^{1,3}

(¹Department of Earth Science, University of Bergen, Allégt. 41, N-5007 Bergen, Norway; ²Department of Geography, University of Bergen, Breiviksveien 40, N-5045 Bergen, Norway; ³Bjerknes Centre for Climate Research, Allégt. 55, N-5007 Bergen, Norway)



Abstract: Three equations derived from a close exponential glacier-climate relationship at the equilibrium-line altitude (ELA) of Norwegian glaciers have been utilized and implemented in a geographical information system (GIS). The first equation enables calculation of the minimum altitude of areas climatically suited for glacier formation at present, and is termed the altitude of instantaneous glacierization (AIG). Equation (2) is based on the 'principle of terrain adaptation', enabling quantification of the glacial buildup sensitivity (GBS) in an area. The third equation calculates the theoretical climatic (instrumental) temperature-precipitation ELA (^cTP-ELA) in presently non-glaciated areas by combining GBS with terrain altitude. The presented approach is primarily intended for palaeoclimatic analyses of former glacial records, and is tested here based on a plot of 122 temperature stations and 197 precipitation stations during the climate normal period 1961–1990 which has been recalculated to sea level using empirical vertical climatic gradients. These data were interpolated in the GIS using an 'inverse square interpolation' routine. Subsequently, the interpolated climatic data were recalculated to the terrain surface using vertical climatic gradients and a digital elevation model (DEM) of southern Norway (resolution 5 × 5 degree minutes/c. 1 km²). The present glacier distribution in southern Norway is reproduced in great detail, and maps showing the modern GBS and ^cTP-ELA in non-glacierized areas of southern Norway are presented. Based on the GBS analysis, four scenarios with ELA depressions of 150 m (average 'Little Ice Age' conditions), 500 m (average coastal Younger Dryas conditions), 1000 m (suggested late Weichselian maximum coastal conditions) and 1500 m are shown.

Key words: Glaciers, equilibrium-line altitude, ELA map, glacial buildup sensitivity, palaeoclimate, climate, geographical information system, GIS, Norway.

Introduction

The glacier equilibrium-line altitude (ELA) is a theoretical line/zone that defines the altitude where the annual accumulation equals the ablation (i.e., net balance, b_n , is zero). Hence, the ELA is regarded as a useful parameter to quantify the influence of climatic variability on glaciers (e.g., Andrews, 1975; Porter, 1975; 1977). In southern Norway, a robust non-linear relationship between observed mean winter precipitation and mean ablation-season temperature at the ELA of 10 Norwegian glaciers has been shown and calculated (Liestøl in Sissons, 1979; Ballantyne, 1989):

$$A = 0.915e^{0.339T} \quad (r^2 = 0.989, P < 0.0001) \quad (1)$$

where A (m water equivalents) is the winter precipitation (defined as the total precipitation between 1 October and 30 April), and T (°C) is the mean ablation-season temperature (1 May to 30 September). In addition to these two main meteorological factors, dry snow can easily be redistributed by wind, and may have a significant effect on the ELA. Due to this influence, Dahl and Nesje (1992) introduced the terms temperature-precipitation ELA (TP-ELA) and temperature-precipitation-wind ELA (TPW-ELA) to distinguish between glacier ELAs reflecting the general winter precipitation and ablation-season temperature in a region (i.e., ice caps), and glacier ELAs being adjusted by either snow deflation

*Author for correspondence (e-mail: oyvind.lie@geol.uib.no)

or snow accumulation (i.e., cirque glaciers) (Figure 1). The regional TP-ELA can thus be regarded as synonymous with the lowest altitude of 'instantaneous glacierization' on a plateau as this term is defined by Ives *et al.* (1975), Dahl and Nesje (1992) and Dahl *et al.* (1997), whereas the TPW-ELA is dependent on local topographic conditions (Figure 1).

In southern Norway, the regional glaciation threshold/ELA rises from an altitude of c. 1200 m at the maritime west coast to c. 2200 m in the continental parts of Jotunheimen and Dovre to the east (e.g., Liestøl, 1967; Østrem *et al.*, 1988). As little is known about the ELA in the presently unglaciated continental areas of east-central southern Norway, it is difficult to estimate the climatic depression required to induce glacierization at a regional scale. To overcome this problem, Dahl *et al.* (1997) formulated a theoretical approach to determine the present ELA in presently non-glaciated areas of east-central southern Norway.

Based on equation (1), three equations describing glacier-climate relations were derived by Lie *et al.* (first paper, this issue). In this study, the equations are utilized in a geographical information system (GIS) to identify the distribution of areas sustaining glaciers by the concept of altitude of instantaneous glacierization' (AIG) at present, and to evaluate the susceptibility to glacier formation in presently non-glaciated areas through the concept of 'glacier buildup sensitivity' (GBS). In addition, a map showing the theoretical 'climatic temperature-precipitation equilibrium-line altitudes' ($^{\circ}$ TP-ELAs) in southern Norway is generated. Based on the GBS model, four scenarios with $^{\circ}$ TP-ELA depressions of 150 m (average 'Little Ice Age' conditions), 500 m (average coastal Younger Dryas conditions; e.g., Nesje and Dahl, 1993), 1000 m (suggested late-Weichselian maximum coastal conditions; e.g., Porter, 1989) and 1500 m are produced. The approach presented here is intended for palaeoclimatic analyses of glacial records. Hence, the equations are 'open-ended', i.e., they allow either the ELA-related terms to be calculated from climate data or winter precipitation to be calculated if former ELAs and ablation-season temperature estimates exist.

Climate at the equilibrium-line altitude

Based on equation (1), Lie *et al.* (first paper, this issue) derived three equations describing glacier-climate relationships at the

ELA. Equation (2) shows how vertical climatic gradients can be combined with equation (1) to calculate the theoretical AIG. As all climate data in the GIS model are recalculated to sea level (datum level), no corrections in the altitude of the climate stations are necessary and the equation can be written as:

$$\text{AIG} = \left[\frac{\ln(0.915) + 0.339t_0 - \ln(p_0)}{\ln(1 + \Delta p) + 0.339 \times \Delta t} \right] \times 100 \quad (2)$$

Equation (2) shows the height in metres above the climate station where conditions are favourable for glacierization based on equation (1), mean summer temperature (t_0), mean winter precipitation (p_0), the adiabatic lapse rate (Δt) and the precipitation-elevation gradient (Δp). As this calculation does not take into account the effect of additional wind deflation and accumulation, the AIG should give the same altitude as any measured TP-ELA, as defined by Dahl and Nesje (1992) (Figure 1). The AIG therefore defines the minimum altitude of the terrain that sustains a plateau glacier in steady-state.

Because the AIG equation does not include a term for terrain altitude, the calculated mean winter precipitation based on equation (1) is allowed to increase into the free atmosphere. Thus, in presently unglaciated areas, the winter precipitation must follow the 'principle of terrain adaptation' (Dahl *et al.*, 1997; Lie *et al.*, first paper, this issue).

Equation (3) calculates the distance between the height where conditions are favourable for glacierization and the terrain, a value which is defined as the glacial buildup sensitivity (GBS). As all climate data are calculated to datum level (sea level) in the model, the GBS equation is slightly modified from Lie *et al.* (first paper, this issue) as only terrain altitude will vary:

$$\text{GBS} = [t_0 - \Delta t \times H] - \left[\ln \left(\frac{p_0 \times (1 + \Delta p)^H}{0.915} \right) \right] \times \frac{100}{\Delta t} \quad (\text{GBS} \neq < 0) \quad (3)$$

where the abbreviations are the same as in equation (2) and H is the terrain altitude (100 m).

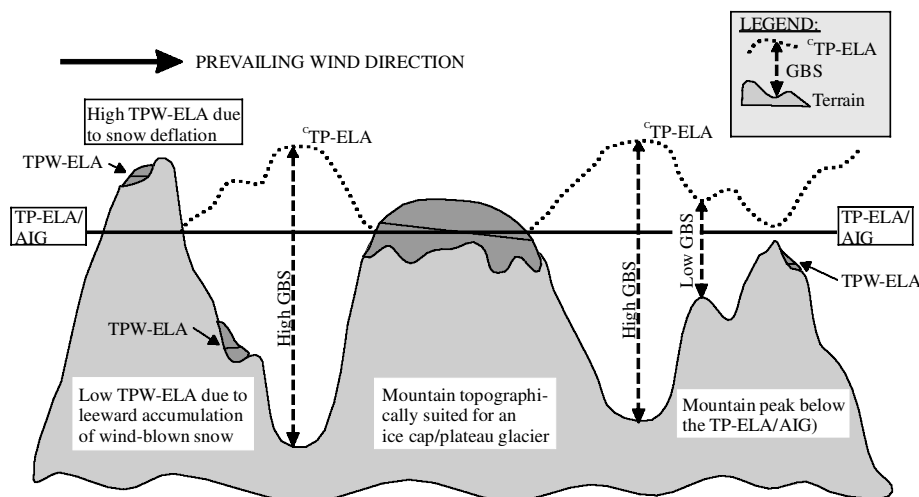


Figure 1 Schematic examples showing the difference between the temperature-precipitation equilibrium-line altitude (TP-ELA) on plateau glaciers, and temperature-precipitation-wind equilibrium-line altitude (TPW-ELA) on cirque glaciers. The altitude of instantaneous glacierization (AIG) is the climatically calculated value of the observed TP-ELA. The glacial buildup sensitivity (GBS) defines the distance between the terrain and the altitude where conditions are favourable for glacier formation when taking the 'principle of terrain adaptation' into account. The climatic temperature-precipitation equilibrium-line altitude ($^{\circ}$ TP-ELA) defines the altitude where conditions are favourable for glacier formation. Note how the GBS and $^{\circ}$ TP-ELA are conditioned by the terrain due to the 'principle of terrain adaptation'. (Modified from Dahl and Nesje, 1992; Dahl *et al.*, 1997.)

As the winter precipitation in the GBS model is controlled by the terrain, the GBS will partly be a function of the topography. Hence, a relatively larger lowering of the ELA is needed to induce glaciation at low altitudes than at high altitudes due to the increase in precipitation with increasing altitude and 'the principle of terrain adaptation' (Figure 1). When the GBS is calculated, the theoretical $^{\circ}\text{TP-ELA}$ can be found by adding the GBS value to the terrain altitude:

$$^{\circ}\text{TP-ELA} = \text{GBS} + (\text{H} \times 100) \quad (4)$$

Implementation of geographical information systems (GIS)

To interpolate between meteorological weather stations and combine the results with terrain altitude, equations (2)–(4) were implemented in a geographical information system (GIS). For this purpose, a raster-based digital elevation model (DEM) covering southern Norway with a cell resolution of 5×5 degree minutes ($c. 1 \text{ km}^2$) was retrieved from the EDC DAAC (2000) (<http://edcdaac.usgs.gov>). The elevation data were resampled into elevation classes of 100 m and a Universal Transverse Mercator (UTM) reference system was attributed to the data. A total of 122 temperature stations and 197 precipitation stations were plotted in the same UTM reference system. All temperature (Aune, 1993) and precipitation (Førland, 1993) data are mean observations of the meteorological normal period 1961–1990. Vertical climatic gradients of $\Delta t = 0.65^{\circ}\text{C } 100 \text{ m}^{-1}$ and $\Delta p = 8\% \text{ } 100 \text{ m}^{-1}$ have been used (see Lie *et al.*, first paper, this issue, and references therein).

The temperature and precipitation data from the climate-station network were first reduced to sea level (datum level) using the vertical gradients (Δt and Δp). Interpolations between the meteorological stations were accomplished by entering the calculated t_0 and p_0 at sea level in the GIS for each station, and an individual cell value for precipitation and temperature distribution at the datum level was established. The interpolations were made at datum level in order to minimize the effect of topography, and in this study inverse-square interpolation was used to calculate precipitation and temperature in areas with no meteorological stations. As each cell of the GIS was assigned a terrain altitude from the DEM and interpolated values for winter precipitation and ablation-season temperature at the datum level, equations (2), (3) and (4) were implemented into the GIS and values for the AIG, GBS and $^{\circ}\text{TP-ELA}$ for each raster cell were calculated.

Results

Altitude of instantaneous glacierization (AIG)

The AIG represents the minimum altitude of glacier occurrence based on any combination of mean winter precipitation and ablation-season temperature without taking wind-redistribution of snow into consideration. To investigate how the model calculates the present glacier distribution in southern Norway (Figure 2A), the DEM was subtracted from the AIG and only areas with an AIG lower than the terrain surface are shown as dark areas (i.e., glaciated areas above the $^{\circ}\text{TP-ELA}$) (Figure 2B). In addition, raster cells with an AIG < 50 m above the terrain surface were included to compensate for the local climatic effect of glaciers (i.e., local cooling of the air and enhanced precipitation over ice).

The close correspondence between the calculated areas supporting glaciers and the observed glacier distribution in southern Norway is striking. All regions of southern Norway supporting glaciers at present are reproduced on the AIG model in great detail.

The model shows areas *above* the ELA (i.e., areas with positive mass balance – the accumulation area), and therefore underestimates glaciated areas by *c.* 40% if an accumulation-area ratio (AAR) of 0.6:1 is assumed for steady-state glaciers (e.g., Andrews, 1975). As the model has no wind-drift routine included, it underestimates glacier occurrence in areas where redistribution of snow is of high importance, i.e., in areas where cirque glaciers dominate (Figure 1).

Glacial buildup sensitivity (GBS) in presently non-glaciated areas

A vector presentation of the GBS results in southern Norway is shown in Figure 3. The data from the GIS analyses has been transformed using a 5×5 cell 'minimum curvature interpolation', and classified into 200 m contour intervals to simplify presentation and readability. Violet to blue colours indicate a high potential for glacier formation, i.e., the $^{\circ}\text{TP-ELA}$ is close to the terrain surface, and only a minor climatic depression is needed to initiate an instantaneous glacierization. Grading towards green/brown, the model indicates an increasingly lower potential for glacier formation. In this case the $^{\circ}\text{TP-ELA}$ is far above the terrain surface, and only a major climatic depression may initiate instantaneous glacierization in these areas (Figure 1).

A clear pattern emerges from the GBS results. Low GBS values are found in the areas west of and along the main watershed in southern Norway. East of the main watershed, the GBS increases rapidly, and the major part of east-central southern Norway has a GBS of more than 1000 m. As expected, the large valley systems of eastern Norway show the highest GBS values (> 2500 m in Figure 3). However, the values are even higher (> 3000 m) in the raster model before vectorizing.

Climatic equilibrium-line altitudes ($^{\circ}\text{TP-ELAs}$) in southern Norway

By adding the calculated GBS to the terrain altitude (equation (4)) based on the DEM, the regional $^{\circ}\text{TP-ELA}$ is yielded (Figure 4). The $^{\circ}\text{TP-ELA}$ results are presented as a 5×5 cell 'minimum curvature' vector plot, with contour intervals of 200 m to increase the readability of the map.

The lowest $^{\circ}\text{TP-ELAs}$ (*c.* 1200–1600 m) are found in western Norway, where the prevailing snow-bearing Atlantic cyclone tracks result in high (orographic) winter precipitation when they reach the mountains some 10–100 km inland of the west coast. Along the west coast the $^{\circ}\text{TP-ELAs}$ are somewhat higher due to lesser orographic effect, while it rises sharply eastwards to 2000–2200 m where the most continental glaciers in southern Norway are found in eastern Jotunheimen and at Dovre, closely resembling the regional ELAs in southern Norway (Liestøl, 1967). In the presently non-glacierized areas of east-central southern Norway, the $^{\circ}\text{TP-ELA}$ continues to rise, reaching more than 2400 m for most of this region, and more than 2600 m in the northernmost part. Towards the Swedish border, the $^{\circ}\text{TP-ELA}$ seems to drop somewhat, mainly due to slightly higher winter precipitation in these areas. The GBS, however, remains high.

The general pattern is a west-to-east increase and south-to-north latitudinal drop in the $^{\circ}\text{TP-ELAs}$. The few major deviations from this pattern are east-central southern Norway, eastern Hardangervidda and the outermost coast of western Norway with higher $^{\circ}\text{TP-ELAs}$ than the surrounding areas, being located in regions of lower precipitation.

Sensitivity tests

When a GBS model is established for a region, the theoretical lowering of the ELA necessary to induce glacierization in areas is given. Assuming a uniform (regional) drop of the $^{\circ}\text{TP-ELA}$, Figure 5 shows the areas above the $^{\circ}\text{TP-ELA}$ in southern Norway during a lowering of 150 m, representative for the 'Little Ice Age',

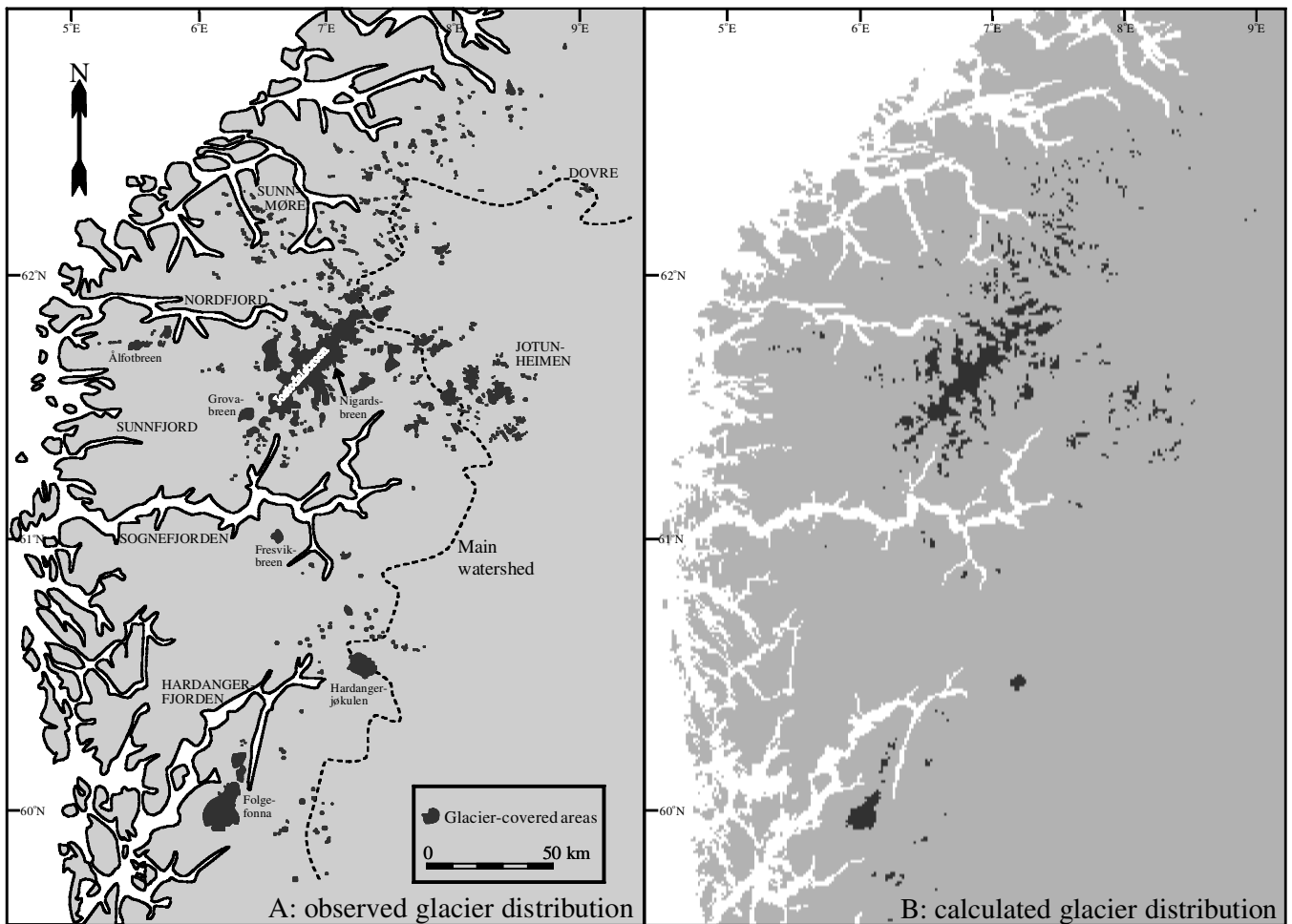


Figure 2 (A) Map showing the observed glacier distribution in southern Norway (based on Østrem *et al.*, 1988). (B) Map showing calculated areas supporting glaciers at present based on the AIG model using meteorological data in a geographical information system (GIS) where the accumulation area of glaciers is indicated as black. In addition, areas lying 50 m below the AIG are incorporated to include local-climatic effects from the glaciers. The AIG is equal to the regional climatic temperature-precipitation equilibrium-line altitude ($^{\circ}\text{TP-ELA}$) in southern Norway when the AIG interferes with the terrain (i.e., $\text{GBS} > 0$; see text for explanation). Note the close correspondence between the observed and calculated glacier distribution in southern Norway.

500 m, representative for the Younger Dryas in coastal areas, 1000 m, suggested to be representative for the Late Weichselian maximum in coastal areas, and 1500 m. In all these scenarios, the glacierization takes place almost entirely along the main watershed or west of it, while only limited areas eastwards are affected by a $^{\circ}\text{TP-ELA}$ drop of 1000 m. With a $^{\circ}\text{TP-ELA}$ lowering of 1500 m, glaciers start to form on a larger scale along the main watershed between east-central southern Norway and Trøndelag and along the watershed between Gudbrandsdalen and Østerdalen. However, the main areas producing ice are located in the western mountains ('Langfjella') and on the central mountain plateaux ('vidder' and 'heier'), especially Hardangervidda, Setesdalsheiene and Ryfylkeheiene, of southern Norway.

The modern distribution of temperature and precipitation in southern Norway strongly indicates that the western mountains along the main watershed will be the source area for an ice-sheet buildup during an initial phase unless a major change in the atmospheric circulation pattern takes place. If temperature alone is to explain the buildup of glaciers in eastern Norway without previously initiating large-scale glacierization along the main watershed, a regional temperature decrease of more than 7°C in eastern Norway is needed compared with the regions along the main watershed. Since such a regional deviation of temperatures is unlikely, considering the relative short distances in southern Norway, changes in the distribution of precipitation must be an important factor for such a situation to occur.

Discussion

The AIG model

The AIG model reproduces in great detail the present distribution of areas supporting glaciers in southern Norway. All major plateau glaciers in southern Norway are shown including areas covered by glaciers on Jostedalsbreen, Folgefonna and Álfotbreen (Figure 2). Plateau glaciers represent TP-ELAs (Figure 1), and a good representation is thus expected. The accumulation zone of Hardangerjøkulen is somewhat smaller than the observed, however, and glaciers around Sunnmøre and north of Hardangerjøkulen are somewhat underestimated in the model.

The apparent modelled occurrence of a glacier in Stølsheimen south of outer Sognefjorden is a result of overestimated precipitation in this region. Snow-bearing winds from the west may follow Sognefjorden longer eastwards than in the surrounding mountain areas before the topography leads to orographic precipitation. Hence, use of precipitation stations along outer Sognefjorden in the AIG model may explain the modelled glacier occurring in Stølsheimen, in addition to effects of redistributions of snow by wind.

The smaller than at present accumulation area on Hardangerjøkulen based on the AIG model is probably related to the circumstances of the nearest meteorological station used in the interpolation. The Finse meteorological station, located *c.* 4 km north-northeast of the glacier, is located in a local 'precipitation shadow'

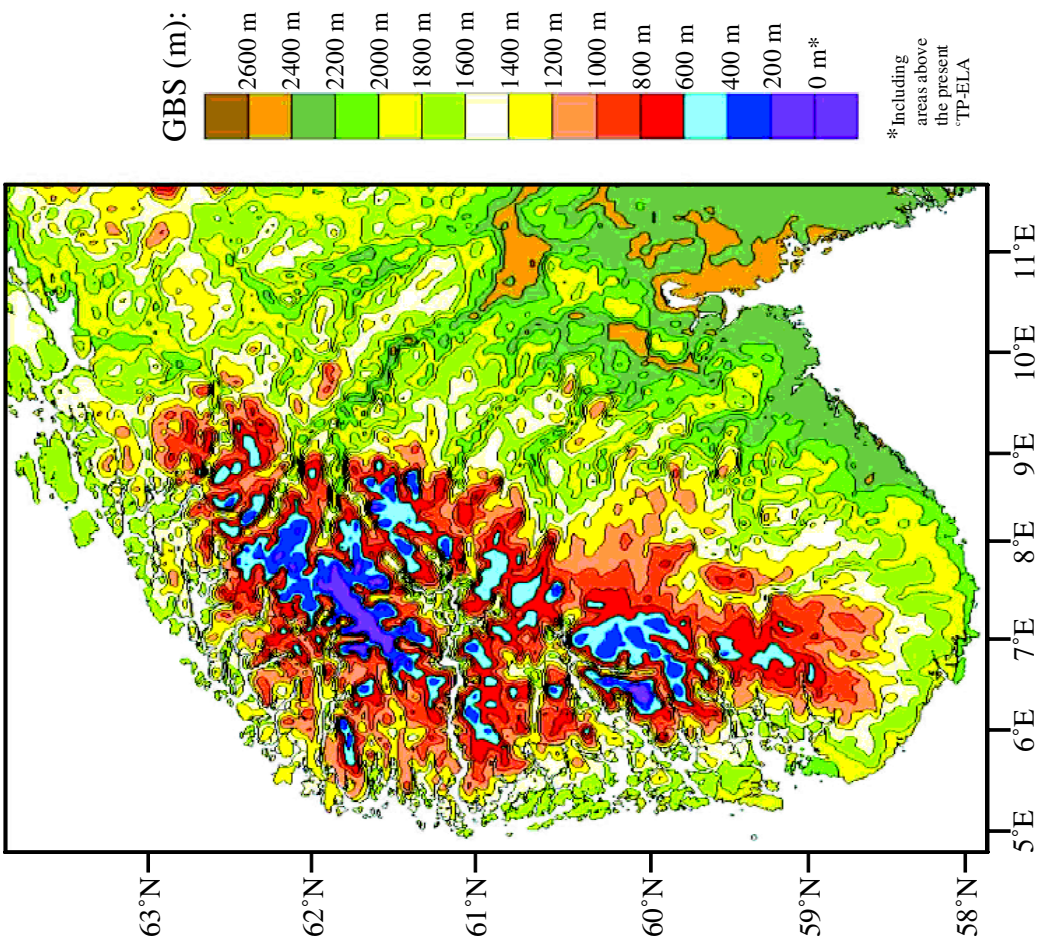


Figure 3 Vectorized map of the glacial buildup sensitivity (GBS) in southern Norway based on a raster model with a minimum curvature of 5×5 degree minutes raster cell filter. Violet to blue areas indicate areas where low $^{\circ}\text{TP-ELA}$ depressions are needed to induce instantaneous glaciation (i.e., the $^{\circ}\text{TP-ELA}$ intersects the terrain), whereas green to brown areas require a significant $^{\circ}\text{TP-ELA}$ depression before steady-state plateau glaciers can be sustained.

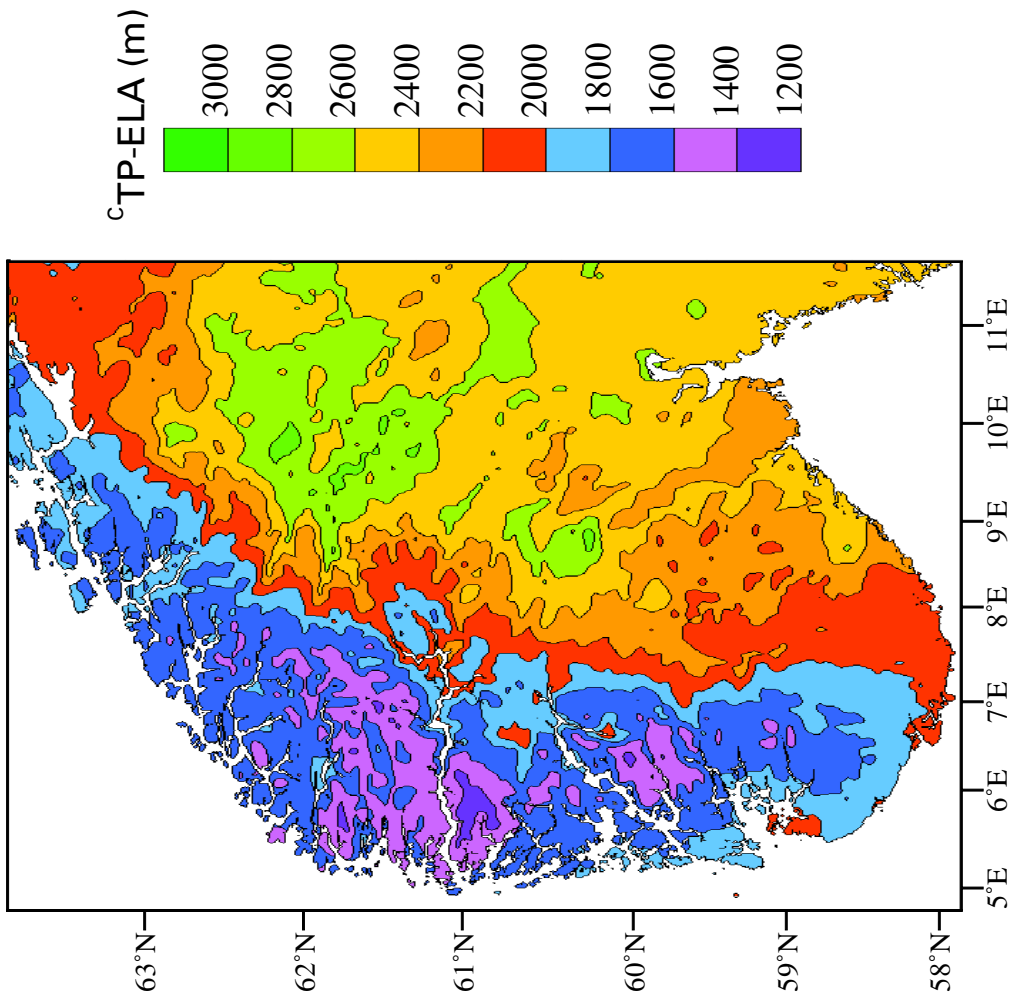


Figure 4 Vectorized map showing the climatic temperature-precipitation equilibrium-line altitudes ($^{\circ}\text{TP-ELA}$) in southern Norway. The $^{\circ}\text{TP-ELA}$ results are presented as a 5×5 cell 'minimum curvature' vector plot with contour intervals of 200 m. Violet and blue colours indicate low altitudes, whereas orange and green colours indicate high altitudes, for the present $^{\circ}\text{TP-ELA}$. Major lakes and rivers are indicated in white.

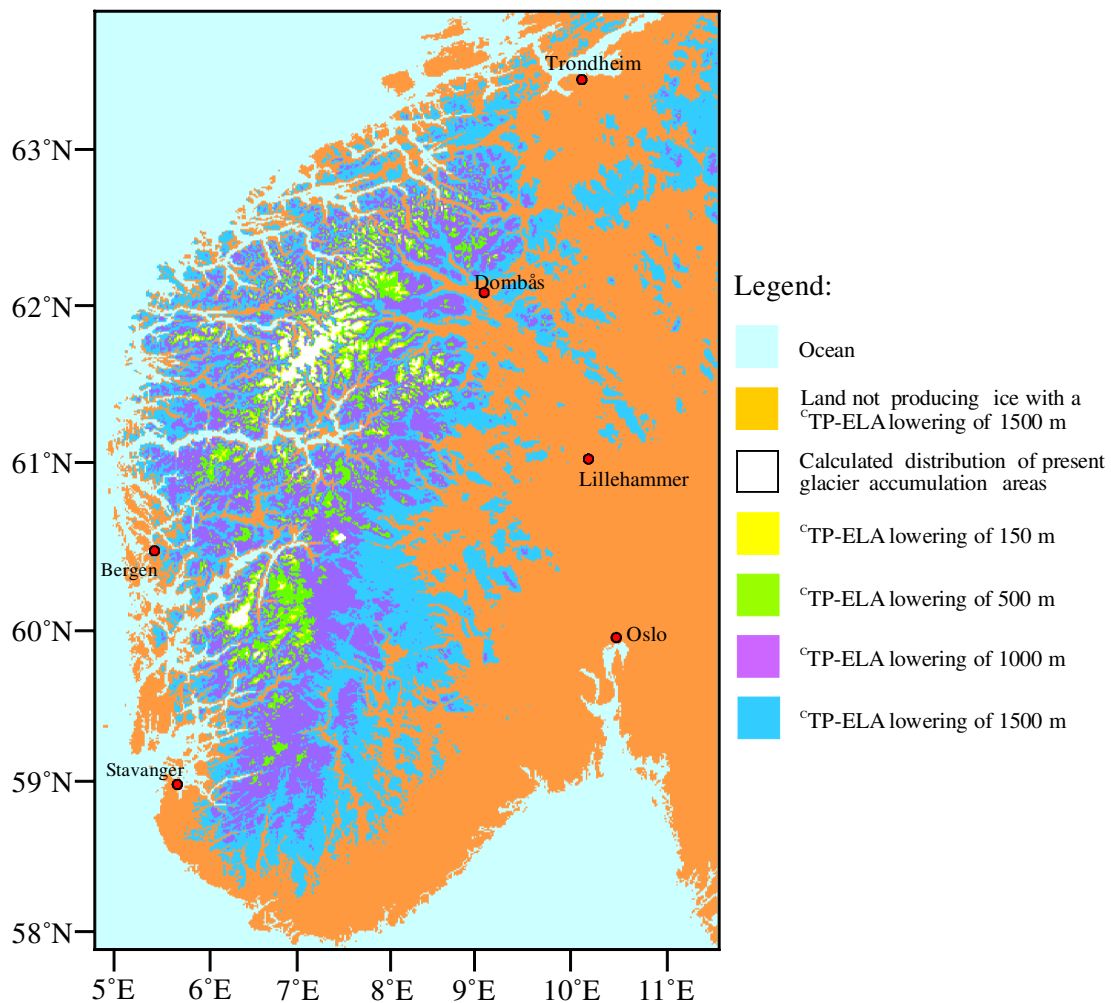


Figure 5 Four sensitivity tests for *uniform* regional $^{\circ}\text{TP-ELA}$ lowerings based on the GBS map in Figure 3. The tests show areas above the $^{\circ}\text{TP-ELA}$ (the accumulation zone) for depressions of 150 (representative for the 'Little Ice Age' in Norway), 500 (representative for the Younger Dryas in coastal areas), 1000 (suggested to be representative for the Late Weichselian maximum in coastal areas) and 1500 m. For all scenarios, the glacierization takes place almost entirely along the main watershed or west of it.

during periods when Hardangerjøkulen receives most of the snow by prevailing west-southwesterly winds. Hence, observations of winter precipitation from Finse underestimate the winter accumulation on Hardangerjøkulen. The same factor may be responsible for the underestimation of glacial extent north of Hardangerjøkulen and in Sunnmøre. One problem in the AIG model is thus the lack of representative meteorological stations in the mountain regions where the glaciers exist.

The most limiting factor for the accuracy of the AIG model is probably the use of general precipitation-elevation and temperature gradients for all of southern Norway. The glaciers exist at high altitude and the climate data are calculated from datum-level (sea-level) interpolations. Hence, local variations in vertical climatic gradients (e.g., Førland, 1979; Green and Harding, 1980) may explain deviations between the calculated and 'real' temperature and precipitation values at the terrain surface. In addition, many areas with glaciers in Norway are dominated by cirque glaciation. Because the AIG model does not take redistribution of snow by wind into account, cirque glaciers are incorrectly located on peaks and ridges in the model instead of in the cirques. This is especially prominent in Sunnmøre. Here the model clearly underestimates the occurrence of glaciers. The situation of these areas are illustrated in Figure 1, where the AIG is close to, but above, the terrain, while a cirque glacier exists below the regional TP-ELA/AIG due to wind-blown snow. This highlights the importance of wind in maintaining glaciers in many regions where cirque glaciers dominate. The success of the AIG model in ident-

ifying most regions where cirque glaciers exist at present, suggests, however, that mountains supporting cirque glaciation need to have their summit altitude at or close to the AIG/ $^{\circ}\text{TP-ELA}$.

The capability of the AIG model in predicting areas with glaciers based on mean ablation-season temperature and winter precipitation alone is remarkably good, and implicitly shows the strong climate signal coupled to the regional distribution of ELAs in southern Norway and hence underscores the potential in using reconstructed palaeo-ELAs to obtain palaeoclimatic information. Moreover, it demonstrates the importance of considering both ablation-season temperature and winter precipitation when deriving palaeoclimate from past glacier variations (Dahl and Nesje, 1996; Nesje *et al.*, 2001).

The GBS and $^{\circ}\text{TP-ELA}$ models

Based on the GBS/ $^{\circ}\text{TP-ELA}$ models, the highest sensitivity for glacierization is in the west-southwestern part of southern Norway, along the main watershed ('Langfjella') and on mountain plateaux such as Hardangervidda, Setesdalsheiene and Ryfylkeheiene (Figures 3 and 5). This geographical distribution mainly reflects factors such as (1) the prevailing atmospheric circulation pattern associated with the dominant west-southwestern (snow-bearing) wind direction in southern Norway, (2) the effects of the warm ocean currents in the North Atlantic/Norwegian Sea on summer and winter temperatures and (3) the topographic north-south barrier ('Langfjella') in Scandinavia. While factor 3 may be regarded as constant, both factors 1 and 2 vary with time. In

Figure 5, areas that theoretically will initiate instantaneous glacierization with $^{\circ}\text{TP-ELA}$ reductions of 150, 500, 1000 and 1500 m are indicated as areas lying above the ELA. The areas producing ice during ELA reductions of 150 and 500 m are located along the main watershed and in regions currently supporting glaciers, with limited areas indicated in Rondane in central southern Norway. Only limited areas in eastern Norway are affected by a $^{\circ}\text{TP-ELA}$ drop of 1000 m based on the present atmospheric circulation pattern, and larger-scale glacierization is initiated along the main watershed towards Trøndelag and along the watershed between Gudbrandsdalen and Østerdalen only with a $^{\circ}\text{TP-ELA}$ lowering of 1500 m (Figure 5). An asymmetric ice-sheet buildup is hence likely based on the evaluation of modern ELA-related terms, being in accordance with recent models of the Fennoscandian ice sheet (e.g., Boulton *et al.*, 2001; Arnold and Sharp, 2002). It is therefore necessary to foresee a major change in circulation patterns to explain a large-scale ice-sheet buildup localized in central southern Norway without previous large-scale buildup from the western mountains. An asymmetric ice growth, radiating from the plateaux along the main watershed in southern Norway, is therefore likely from the evaluation of present ELAs in the region.

When using the GBS/ $^{\circ}\text{TP-ELA}$ models, some limitations of the approach must be taken into account.

- (1) The models are not better than the data that they are based on. A main limitation is thus the geographical distribution of representative data.
- (2) As the basis for all the equations in the models, equation (1) is based on smaller cirque glaciers and ice caps; ice sheets may have impacts on the local climate in ways the models do not take into account.
- (3) The glaciated areas in Figure 2B and the various scenarios in Figure 5 only indicate areas that will lay within the accumulation zone (i.e., areas having a positive mass balance) of (plateau) glaciers at present and for the different climate scenarios reflected in the $^{\circ}\text{TP-ELA}$ lowerings. Hence, the glaciated areas will be 30–40% larger if an AAR of 0.6–0.7 for glaciers in steady-state is assumed.
- (4) The GBS/ $^{\circ}\text{TP-ELA}$ approach reflects instantaneous glacierization and cannot be used uncritically on downwasting ice sheets that were not in equilibrium with climatic conditions (i.e., the Younger Dryas Fennoscandian ice sheet).
- (5) The presented GBS/ $^{\circ}\text{TP-ELA}$ scenarios assume a uniform $^{\circ}\text{TP-ELA}$ lowering, which is unlikely, especially for the largest $^{\circ}\text{TP-ELA}$ depressions. If larger ice masses are formed, the regional circulation patterns will change, and the assumption of a linear $^{\circ}\text{TP-ELA}$ lowering is invalid.

The $^{\circ}\text{TP-ELA}$ map

The $^{\circ}\text{TP-ELA}$ map shows a distinct general rise from west to east, as well as an expected drop from south to north. The western parts of Norway with glaciers at present have $^{\circ}\text{TP-ELAs}$ of 1200 m, increasing to 2200 m in eastern Jotunheimen and at Dovre. East-central southern Norway and eastern parts of Hardangervidda have the highest $^{\circ}\text{TP-ELAs}$ in southern Norway, indicated with green colours in Figure 4. These areas have very low winter precipitation as they lie in the ‘precipitation shadow’ of the western mountains in addition to having high summer temperatures. The outermost coast of western Norway only receives about 50% of the winter precipitation compared with the mountain areas some few tens of kilometres farther inland due to lower orographic effect. The zone of higher $^{\circ}\text{TP-ELAs}$ along the coast of western Norway is very important for the reconstruction and interpretation of former glacier ELAs, especially those of suggested Younger Dryas age in presently non-glaciated areas.

The approach in palaeoclimatic investigations

The equations presented in Lie *et al.* (first paper, this issue) and incorporated into GIS models here are ‘open-ended’, encompassing the three variables winter precipitation, summer temperature and an ELA-related term. The equations being ‘open-ended’ means that they can be used if two of these variables are known, calculating the third. Here, observed p_0 and t_0 have been used to calculate the present AIG, GBS and $^{\circ}\text{TP-ELA}$ of southern Norway and to describe the areas that have climatic potential to support glaciers at present without the impact of wind-blown snow.

By comparing trend surfaces based on reconstructed ELAs with the calculated (modern) $^{\circ}\text{TP-ELA}$, different slopes of ELA surfaces can be calculated. In southern Norway a relationship between changes in the North Atlantic atmospheric circulation, expressed through the ‘North Atlantic Oscillation’, and regional mass-balance variations, has been identified (Nesje *et al.*, 2000). It may thus be possible to associate varying trend surfaces of Holocene ELA variations to changes in the atmospheric circulation pattern. Moreover, if the distribution of time-synchronous records of glacier variations and temperature are known, the model can calculate the precipitation distribution and gradients that explains the observed ELAs.

The model allows evaluation of wind-blown snow on cirque glaciers as demonstrated by Lie *et al.*, (first paper, this issue). By comparing the present TPW-ELA of a cirque glacier with the regional $^{\circ}\text{TP-ELA}$ map, the deviation between the observed TPW-ELA and the calculated $^{\circ}\text{TP-ELA}$ expresses the difference between the regional and local climate including redistribution of snow by wind. As the annual correlations of calculated AIG on cirque glaciers are similar to plateau glaciers compared with observed net mass-balance measurements (Lie *et al.*, first paper, this issue), it can be deduced that the deviation between local and regional ELAs can be set as a relatively constant value through time, hence making regionalized climate reconstructions from cirque glaciers possible.

Conclusions

(1) Three equations derived from a close exponential glacier-climate relationship at the ELA of Norwegian glaciers (Lie *et al.*, first paper, this issue) have been combined with a digital elevation model (DEM) and interpolated meteorological data (mean ablation-season temperature and winter precipitation) from southern Norway in a raster-based geographical information system (GIS).

(2) The AIG model reproduces in great detail the modern distribution of glaciers in southern Norway (Figure 2). In a few areas, the extent of glaciers are underestimated, while in one case the glacier extent is overestimated. The main reasons for these deviations are likely due to lack of representative meteorological stations. Also, the AIG model does not take into account redistribution of (dry) snow by wind. However, it seems that mountains supporting cirque glaciation in general must be close to the AIG/ $^{\circ}\text{TP-ELA}$.

(3) The close agreement between the observed and calculated distribution of glaciers based on meteorological data in southern Norway demonstrates the potential of using reconstructed glacier variations as a palaeoclimate proxy. It also shows the importance of considering both temperature and precipitation in palaeoclimate reconstructions based on glacial evidence (Dahl and Nesje, 1996).

(4) The potential glacier buildup sensitivity in southern Norway is shown in Figure 3. Areas with low GBS values are found to the west of and along the main watershed in the vicinity of modern glaciers. Eastwards the GBS increases significantly, and the $^{\circ}\text{TP-ELA}$ lowering necessary to induce glacierization in much of

east-central southern Norway generally is in excess of 1000 m. Even mountain plateaux do not produce large amounts of glacier ice with a $^{\circ}\text{TP-ELA}$ lowering of 800–1000 m in this region, and over the large valley systems of eastern Norway the GBS commonly exceeds 2500 m.

(5) By combining the GBS model with terrain altitude, the $^{\circ}\text{TP-ELA}$ can be calculated for presently glaciated and non-glaciated areas (Figure 4). The lowest $^{\circ}\text{TP-ELAs}$ of 1200 to 1600 m are found in the western mountain areas, where the prevailing snow-bearing cyclone tracks result in high orographically increased winter precipitation. Along the coast to the west of these mountains, the $^{\circ}\text{TP-ELAs}$ are somewhat higher. They rise sharply towards the east, reaching altitudes of *c.* 2200 m in eastern Jotunheimen and at Dovre, where the most continental glaciers in southern Norway are located. In the non-glaciated areas of eastern Norway, the $^{\circ}\text{TP-ELAs}$ are between 2400 to 2800 m over most of the region, with only limited areas having values lower than 2400 m. Areas with $^{\circ}\text{TP-ELAs}$ consistently above 2600 m are found in the northern part of eastern Norway.

(6) Four sensitivity tests were carried out in order to model the accumulation areas that result from uniform lowerings of the $^{\circ}\text{TP-ELA}$ of 150 m (representative for the 'Little Ice Age'), 500 m (representative for the Younger Dryas in coastal areas), 1000 m (suggested to be representative for the Late Weichselian maximum in coastal areas) and 1500 m (Figure 5). In all these scenarios, the glacierization takes place almost entirely along the main watershed and to the west of it. Only limited areas east of the main watershed are affected by $^{\circ}\text{TP-ELA}$ lowerings of 1000 m. Large-scale glaciation is initiated along the main watershed between east-central southern Norway and Trøndelag and along the watershed between Gudbrandsdalen and Østerdalen with a $^{\circ}\text{TP-ELA}$ lowering of 1500 m or more. With the prevailing atmospheric circulation patterns this strongly indicates west/southwestern source areas for any large-scale glacier buildup in southern Norway, with an initial asymmetric shape of the ice sheet in southern Norway.

(7) The model gives a theoretical and methodological foundation to interpret regional changes and variations in ELAs as a consequence of varying distribution of precipitation if data on ablation-season temperature is available.

Acknowledgements

The Digital Elevation Model was retrieved from the EROS Data Center – Distributed Active Archive Center (EDC DAAC). Jan Roar Sulebak kindly rectified, warped and created the reference system for the DEM. Mel Reasoner and an anonymous referee provided helpful comments to improve the clarity of this manuscript. This paper is a contribution from NORPAST, a coordinated Norwegian palaeoclimate project funded by the Norwegian Research Council (NFR) and from the Bjerknes Centre for Climate Research.

References

- Andrews, J.T.** 1975: *Glacial systems. An approach to glaciers and their environments*. North Scituate: Duxbury Press.
- Arnold, N.** and **Sharp, M.** 2002: Influence of glacier hydrology on the dynamics of a large Quaternary ice-sheet. *Journal of Quaternary Science* 7, 109–24.
- Aune, B.** 1993: *Air temperature normals, normal period 1961–1990*. Det norske meteorologiske institutt – klimaavdelingen. Rapport 02/93, Klima.
- Ballantyne, C.K.** 1989: The Loch Lomond readvance on the Island of Skye, Scotland: glacier reconstruction and paleoclimatic implications. *Journal of Quaternary Science* 4, 95–108.
- Boulton, G.S., Dongelmans, P., Punkari, M.** and **Broadgate, M.** 2001: Palaeoglaciology of an ice sheet through a glacial cycle: the European ice sheet through the Weichselian. *Quaternary Science Reviews* 20, 591–625.
- Dahl, S.O.** and **Nesje, A.** 1992: Paleoclimatic implications based on equilibrium-line altitude depressions of reconstructed Younger Dryas and Holocene cirque glaciers in inner Nordfjord, western Norway. *Palaeogeography, Palaeoclimatology, Palaeoecology* 94, 87–97.
- 1996: A new approach of calculating Holocene winter precipitation by combining glacier equilibrium-line altitudes and pine-tree limits; a case study from Hardangerjøkulen, central southern Norway. *The Holocene* 6, 381–98.
- Dahl, S.O., Nesje, A.** and **Øvstedal, J.** 1997: Cirque glaciers as morphological evidence for a thin Younger Dryas ice sheet in east-central southern Norway. *Boreas* 26, 161–80.
- Førland, E.** 1979: Precipitation and topography. *Klima* 2, 3–24.
- 1993: *Precipitation normals, normal period 1961–1990*. Det norske meteorologiske institutt – klimaavdelingen. Rapport 39/93, Klima.
- Green, F.H.W.** and **Harding, R.J.** 1980: The altitudinal gradients of air temperature in southern Norway. *Geografiska Annaler* 62A, 29–36.
- Ives, J.D., Andrews, J.T.** and **Barry, R.G.** 1975: Growth and decay of the Laurentide ice sheet and comparison with Fenno-Scandinavia. *Naturwissenschaften* 62, 118–25.
- Liestøl, O.** 1967: Storbreen glacier in Jotunheimen, Norway. *Norsk Polarinstitutt skrifter* 141, 1–63.
- Nesje, A.** and **Dahl, S.O.** 1993: Lateglacial and Holocene glacier fluctuations and climate variations in western Norway: a review. *Quaternary Science Reviews* 12, 255–61.
- Nesje, A., Lie, Ø.** and **Dahl, S.O.** 2000: Is the North Atlantic Oscillation reflected in Scandinavian glacier mass balance records? *Journal of Quaternary Science* 15, 587–601.
- Nesje, A., Matthews, J.A., Dahl, S.O., Berrisford, M.S.** and **Andersson, C.** 2001: Holocene glacier fluctuations of Flatebreen and winter-precipitation changes in the Jostedalbreen region, western Norway, based on glaciolacustrine sediment records. *The Holocene* 11, 267–80.
- Østrem, G., Dale Selvig, K.** and **Tandberg, K.** 1988: *Atlas of glaciers in South Norway*. Norges vassdrags- og energiverk, vassdragsdirektoratet. Meddelelse 61, fra Hydrologisk avdeling.
- Porter, S.C.** 1975: Equilibrium-line altitudes of late Quaternary glaciers in the Southern Alps, New Zealand. *Quaternary Research* 5, 27–47.
- 1977: Present and past glaciation threshold in the Cascade Range, Washington, USA. Topographic and climatic controls, and paleoclimatic implications. *Journal of Glaciology* 18, 101–16.
- 1989: Some geological implications of average Quaternary conditions. *Quaternary Research* 32, 245–61.
- Sissons, J.B.** 1979: Palaeoclimatic inferences from former glaciers in Scotland and the Lake District. *Nature* 278, 518–21.